Inorganic Chemistry

Article

pubs.acs.org/IC

Functionalized Pentamolybdodiphosphate-Based Inorganic–Organic Hybrids: Synthesis, Structure, and Properties

Xiao-Min Li,[†,‡] Ya-Guang Chen,*[,†] Chunnian Su,[§] Shi Zhou,[†] Qun Tang,[†] and Tian Shi[†]

[†]Department of Chemistry, Northeast Normal University, Changchun, Jilin 130024, P. R. China

[‡]Department of Chemistry, Yili Normal University, Yining, Xingjiang 835000, P. R. China

[§]Jilin Medical College, Jilin City 132100, P. R. China

Supporting Information

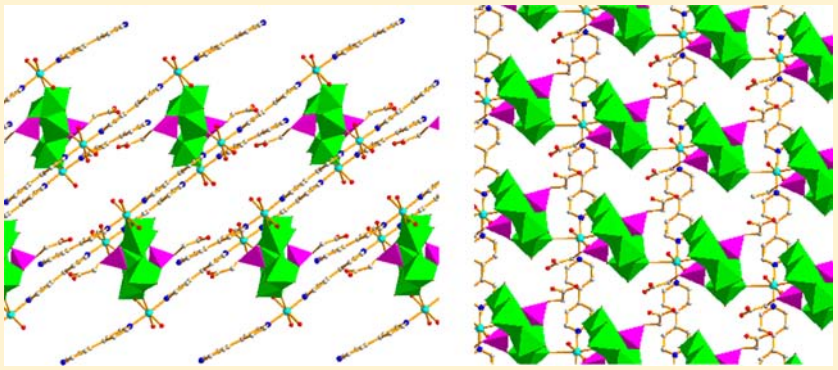

ABSTRACT: Three inorganic–organic hybrid compounds based on functionalized pentamolybdodiphosphonopropionate anion $[(HO_2CC_2H_4PO_3)_2Mo_5O_{15}]^{4-}$, $[Co_3(bipy)_4(H_2O)_6\{(HO_2CC_2H_4PO_3)_2Mo_5O_{15}\}_2]\cdot(H_2bipy)_2\cdot 18H_2O$ (**1**), $[Fe_3(bipy)_4(H_2O)_6\{(HO_2CC_2H_4PO_3)_2Mo_5O_{15}\}_2]\cdot(H_2bipy)_2\cdot 18H_2O$ (**2**), and $[Cu(bipy)(H_2O)_2\{(HO_2CC_2H_4PO_3)_2Mo_5O_{15}\}]\cdot(H_2bipy)\cdot 4H_2O$ (**3**), where bipy = 4,4′-bipyridine, have been successfully synthesized at different pH values in aqueous solutions. In compound **1**, $[(HO_2CC_2H_4PO_3)_2Mo_5O_{15}]^{4-}$ acts as a tridentate ligand and coordinates to the Co^{2+} ions of trimeric complex cations $[Co_3(bipy)_4(H_2O)_6]^{6+}$ forming a layer. In **3** $[(HO_2CC_2H_4PO_3)_2Mo_5O_{15}]^{4-}$ acts as a bidentate ligand and coordinates to the Cu^{2+} ions of complex chains $[Cu(bipy)(H_2O)_2]_n^{2n+}$, forming a different layer from that in **1**. The three compounds were characterized by elemental analysis, IR spectra, and TGA. In addition, their fluorescent properties and magnetic properties have also been investigated.

INTRODUCTION

Since the structure of pentamolybdodiphosphate ion $[(HO\text{-}PO_3)_2Mo_5O_{15}]^{4-}$ was determined by Strandberg in 1973,[1] many derivatives of the Strandberg anion have been reported in the last 40 years, for example, organophosphonate derivatives ($[(RPO_3)_2Mo_5O_{15}]^{4-}$, R = CH_3, C_2H_5, Ph, $NH_2C_2H_4$, $CH_3CH(NH_2)$, $CH_3CH(CH_3)CH(NH_2)$, $CH_2C_6H_4NH_2$, S-$(CH_2CH_2)_2NHCH_2$, crown ether), phosphite derivative ($[(HPO_3)_2Mo_5O_{15}]^{4-}$),[2] phosphonocarboxylate derivatives ($[(O_2CCH_2PO_3)_2Mo_5O_{15}]^{6-}$, and $[(O_2CC_2H_4PO_3)_2Mo_5$ $shyO_{15}]^{6-}$),[3] organodiphosphonates derivatives ($\{(O_3PRPO_3)\text{-}Mo_5O_{15}\}_n^{4n-}$ R = $(CH_2)_x$, x = 2–5, C_6H_4, Ph–Ph)[4] or the derivatives modified by metal complex or metal ion.[5] The $[(HOPO_3)_2Mo_5O_{15}]^{4-}$ polyoxoanion consists of a chiral ring of five alternating edge- and corner-sharing MoO_6 octahedra (point group C_2) capped above and below by phosphate groups. Generally, in the organophosphonate derivatives ($[(RPO_3)_2Mo_5O_{15}]^{4-}$, the pending R group does not participate in coordination to the transition metal center.[2,3b] Modification of the Strandberg anion by metal complex or metal ion via coordination of the oxygen atoms of molybdate or phosphate results in chain or network structures.[5] In Zubieta's materials[4] with organodiphosphonates replacement of organodiphosphonates for phosphates leads to polyoxoanion chain, the pentamolybdate units in the polyoxoanion chain and the organic chelating ligands coordinate to M complexes, forming a series of compounds with three-dimensional structure. Recently, Zubieta et al. gave a review on the structure chemistry of this kind of materials.[6] In addition, the presence of terminal carboxyl functional groups on each side of the polyanion in $[(HO_2CCH_2PO_3)_2Mo_5O_{15}]^{4-}$ renders this species highly attractive for further decoration with organic molecules or coordination to metal ions and for construction of multidimensional structure. To date, a study on this kind of materials is rather rare.[3c]

On the other hand, most of the metal–organic derivatives with multidimensional structure were obtained with a hydrothermal synthesis method. The hydrothermal synthesis method has some advantages, for example, increasing solubility and

Received: July 4, 2013
Published: September 10, 2013

dx.doi.org/10.1021/ic401726a | Inorg. Chem. 2013, 52, 11422–11427

raising reactivity, but special apparatus and high energy consumption are necessary. In contrast, aqua solution synthesis is more consistent with eco-friendly and low-carbon idea. In order to explore the reactivity of phosphonocarboxylate derivatives of pentamolybdodiphosphate anion, we choose transition metal ions Co^{2+}, Fe^{2+}, and Cu^{2+}, phosphonopropionic acid, and 4,4′-bipyridine as starting materials and carry out the reaction in aqua solution. Three derivatives of pentamolybdodiphosphonopropionate $[Co_3(bipy)_4(H_2O)_6\{(HO_2CC_2H_4PO_3)_2Mo_5O_{15}\}_2]\cdot(H_2bipy)_2\cdot 18H_2O$ (**1**), $[Fe_3(bipy)_4(H_2O)_6\{(HO_2CC_2H_4PO_3)_2Mo_5O_{15}\}_2]\cdot(H_2bipy)_2\cdot 18H_2O$ (**2**), and $[Cu(bipy)(H_2O)_2\{(HO_2CC_2H_4PO_3)_2Mo_5O_{15}\}]\cdot(H_2bipy)\cdot 4H_2O$ (**3**) were obtained. Herein their syntheses, structures, and properties are reported.

EXPERIMENTAL SECTION

Materials and Instruments. All reactants and solvents were of commercially available grade and used without any further purification. IR spectra in KBr pellets were recorded in the range 400−4000 cm^{-1} with a Magna-560 FT/IR spectrophotometer. Elemental analyses (C, H, and N) were performed on a Perkin-Elmer 2400 CHN elemental analyzer, and those of Mo, Co, Fe, and Cu were carried out with a Leaman ICP spectrometer. Thermogravimetric analyses were carried out using a NETZSCH STA 449F3 instrument with a heating rate of 10 °C·min^{-1} under a nitrogen atmosphere. X-ray powder diffraction (XRPD) patterns were recorded on a D/MAX-IIIC diffractometer with Cu Kα radiation (λ = 1.5418 Å). Photoluminescence spectra were measured with a pure solid sample at room temperature using a SPEX FL-2T2 instrument with a 450 W xenon lamp monochromatized by double grating (1200). Variable-temperature dc magnetic susceptibility measurements were performed on polycrystalline samples in an applied magnetic field of 1000 Oe over the temperature range 2.0−300 K using a Quantum Design XL-5 SQUID magnetometer.

Synthesis. *Synthesis of $[Co_3(bipy)_4(H_2O)_6\{(HO_2C_3H_4PO_3)_2Mo_5O_{15}\}_2]\cdot(H_2bipy)_2\cdot 18H_2O$ (1).* Into 30 mL of distilled water was dissolved $Na_2MoO_4\cdot 2H_2O$ (0.073 g, 0.3 mmol) and $(HO)_2P(O)CH_2CH_2COOH$ (0.015 g, 0.1 mmol), the solution was stirred for 20 min, and then $(CH_3COO)_2Co\cdot 4H_2O$ (0.025 g, 0.1 mmol) and $C_{10}H_8N_2\cdot 2H_2O$ (0.019 g, 0.1 mmol) were added with stirring. The pH of the resulting solution was adjusted with a 0.1 mol·L^{-1} HNO_3 solution to 5.0; the mixture was heated 80 °C over a period of 2 h and filtered. The filtrate was allowed to evaporate in air at room temperature. After 2 weeks, brown-red block crystals of **1** were isolated from the filtrate with a yield of 38% based on molybdenum. Anal. Calcd for $C_{72}H_{116}N_{12}Co_3O_{74}Mo_{10}P_4$ (M_r = 3593.43): C, 24.04; H, 3.23; N, 4.67; Co, 4.92; Mo, 26.70. Found: C, 24.00; H, 3.18; N, 4.64; Co, 4.96; Mo, 26.74. IR (KBr pellet, cm^{-1}): 3402(br), 3084(m), 3054(m), 2911(m), 1729(m), 1642(m), 1600(s), 1535(m), 1487(s), 1410(m), 1338(w), 1244(m), 1109(s), 1040(m), 984(s), 922(s), 812(s), 684(m), 666(s) 552(m), 410(w).

Synthesis of $[Fe_3(bipy)_4(H_2O)_6\{(HO_2C_3H_4PO_3)_2Mo_5O_{15}\}_2]\cdot(H_2bipy)_2\cdot 18H_2O$ (2). Preparation of **2** was similar to that of **1** except that $FeSO_4\cdot(NH_4)_2SO_4\cdot 6H_2O$ (0.039 g, 0.1 mmol) was used instead of $(CH_3COO)_2Co\cdot 4H_2O$, and the pH of the resulting solution was adjusted to 2.8. After 1 week, dark-brown block crystals of **2** were isolated from the filtrate with a yield of 36% based on molybdenum. Anal. Calcd for $C_{72}H_{116}N_{12}Fe_3O_{74}Mo_{10}P_4$ (M_r = 3584.17): C, 24.11; H, 3.24; N, 4.69; Fe, 4.67; Mo, 26.77. Found: C, 24.08; H, 3.20; N, 4.65; Fe, 4.70; Mo, 26.81. IR (KBr, pellet, cm^{-1}): 3437(br), 3386(br), 2950(m), 1720(m), 1639(m), 1600(s), 1500(s), 1411(m), 1244(m), 1107(s),1040(m), 983(s), 922(s), 810(s), 665(s), 551(m).

Synthesis of $[Cu(bipy)(H_2O)_2\{(HO_2CC_2H_4PO_3)_2Mo_5O_{15}\}]\cdot(H_2bipy)\cdot 4H_2O$ (3). Preparation of **3** was similar to that of **1** except that $(CH_3COO)_2Cu\cdot H_2O$ (0.020 g, 0.1 mmol) was used instead of $(CH_3COO)_2Co\cdot 4H_2O$, and the pH was 3.0, After 1 week, pale blue block crystals of **3** were isolated from the filtrate with a yield of 35% based on molybdenum. Anal. Calcd for $C_{26}H_{37}CuMo_5N_4O_{31}P_2$ (M_r = 1506.79): C, 20.71; H, 2.46; N, 3.72; Cu, 12.65; Mo, 31.84. Found: C, 20.67; H, 2.42; N, 3.68; Cu, 12.70; Mo, 31.89. IR (KBr, pellet, cm^{-1}): 3480(br), 3363(br), 3110(m), 3069(m), 2920(m), 2853(m), 1717(m), 1635(s), 1600(s), 1500(m), 1420(m), 1386(m), 1215(m), 1107(s), 986(s), 918(s), 802(s), 669(s), 551(m), 516(m), 484(m).

X-ray Crystallography. Single-crystal samples of **1** and **3** with suitable size were sealed in capillaries. X-ray diffraction data were collected on a Gemini R Ultra diffractometer with graphite monochromatic Mo Kα radiation (λ = 0.71073 Å) at T = 293 K with ω scans. Multiscan absorption corrections were applied. Structures were solved by direct methods and refined by full-matrix least-squares on F^2 with the SHELXTL-97 program package.[7] Positions of hydrogen atoms on the carbon atoms were calculated theoretically. A summary of the crystallography data and refinement parameters for compounds **1** and **3** is listed in Table 1.

Table 1. Crystal Parameters and Structure Refinement Data for 1 and 3

	1	3
formula	$C_{72}H_{64}Co_3Mo_{10}N_{12}O_{74}P_4$	$C_{26}H_{37}CuMo_5N_4O_{31}P_2$
M_r	3541.43	1506.79
cryst syst	triclinic	triclinic
space group	*P*-1	*P*-1
a (Å)	12.476(5)	9.722(5)
b (Å)	12.715(5)	11.116(5)
c (Å)	20.931(5)	20.960(5)
α (deg)	74.508(5)	88.945(5)
β (deg)	86.133(5)	86.593(5)
γ (deg)	76.031(5)	70.698(5)
V (Å^3)	3105.1(19)	2134.0(15)
Z	1	2
D_c (g·cm^{-3})	1.91	2.345
μ, mm^{-1}	1.519	2.100
F(000), e	1763.0	1476.0
no. of reflns measd	16710	13624
no. of reflns unique	6167	8157
R_{int}	0.0645	0.0245
R indices [$I \geq 2\sigma(I)$]	R_1 =0.0740, wR_2 = 0.1788	R_1 = 0.0416, wR_2 = 0.0980
R indices (all date)	R_1 = 0.1508, wR_2 = 0.2045	R_1 = 0.0465, wR_2 = 0.1007
GOF on F^2	1.017	1.032
CCDC No	945266	945267

RESULTS AND DISCUSSION

Crystal Structure Description. *$[Co_3(bipy)_4(H_2O)_6\{(HO_2CC_2H_4PO_3)_2Mo_5O_{15}\}_2]\cdot(Hbipy)_2\cdot 18H_2O$ (1).* Single-crystal structural analysis reveals that the asymmetric unit of compound **1** contains 1 $[(HO_2CC_2H_4PO_3)_2Mo_5O_{15}]^{4-}$ polyoxoanion (abbreviation $(RP)_2Mo_5$), 1.5 Co^{2+} ions, 3 4,4′- bipyridine (bipy) molecules, and 24 water molecules (Figure S1, Supporting Information).

Anion $[(HO_2CC_2H_4PO_3)_2Mo_5O_{15}]^{4-}$ consists of a ring of five MoO_6 octahedra with four edge junctions and one corner junction and two propyloic phosphonates which are bound via their phosphonate on opposite sides of the ring; propyloic groups like two arms stick out the Mo_5 ring. Mo−O distances can be grouped into four sets: Mo−μ_3-O_b 2.190(8)−2.431(9) Å, Mo−μ_2-O_b 1.880(8)−1.955(8) Å, Mo−Ot (terminal) 1.678(9)−1.712(9) Å, and Mo−Ot′ (terminal oxygen coordinated to Co^{2+} ions) 1.717(8)−1.735(8) Å. The P−C bond lengths are 1.792(12) and 1.782(13) Å, the bond angle of O−P−O is 106.8(5)−112.9(5)°, and all data are consistent with

dx.doi.org/10.1021/ic401726a | Inorg. Chem. 2013, 52, 11422−11427

that in ref 1 except the Mo−Ot′ bond lengths which are elongated due to coordination to Co^{2+} ions.

$(RP)_2Mo_5$ anion of **1** acts as a tridentate ligand and coordinates to three Co^{2+} ions via the three terminal oxygen atoms (O6, O14, O19) (Figure S1, Supporting Information). The propyloic groups do not take part in the coordination to the Co ions. All of the Co^{2+} ions display a slightly distorted octahedral geometry (Table S1, Supporting Information, Co−O/N bond lengths). The coordination atoms of Co1 ion are two terminal oxygen atoms (O14, O19′) of two $(RP)_2Mo_5$ anions, two coordination water molecules (O5 and O9), and two nitrogen atoms (N2, N4) of two bipyridine molecules. Co2 ion is coordinated with two terminal oxygen atoms (O6, O6′) of two $(RP)_2Mo_5$ anions, two coordination water molecules (O2 and O2′), and two bipyridine nitrogen atoms (N1, N1′).

In the asymmetric unit of **1** there are three bipy molecules, but only two of them act as ligands to connect with Co ions; the other one is an independent protonated molecular ion. Bipy1 as a monodentate ligand binds Co1 ion with its N4 atom; bipy2 as a bidentate bridging ligand connects Co1 ion with its N2 atom and Co2 ion with N1 atom. Co2 ion is a symmetric center, and the other two bipys and one Co1 ion are obtained by inversion operation, so that a trimeric complex cation $[Co_3(bipy)_4]^{6+}$ is formed (Figure 1)

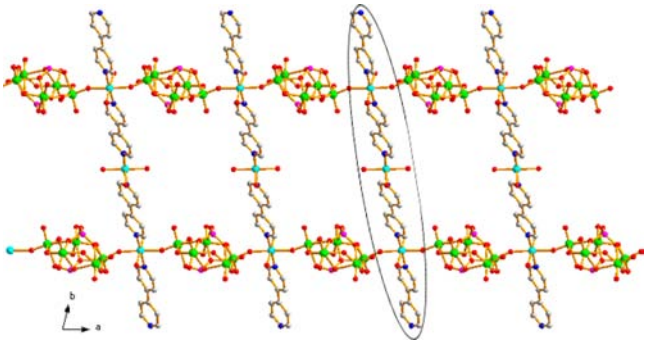

Figure 1. Ball and stick representation of the ladder-like chain in **1**; the trimeric cation is circled by elliptic line. Hydrogen atoms, propyloic groups, and lattice water molecules are omitted for clarity.

Two $(RP)_2Mo_5$ anions coordinate to the Co1 ions of two trimers with terminal oxygen atoms, forming a 1-D ladder chain stretching along the *a* axis (Figure 1). In turn, Co2 ion of the trimer on the ladder chain (1) accepts two terminal oxygen atoms of the $(RP)_2Mo_5$ on the two other ladder chains (2, 3); simultaneously, two terminal oxygen atoms of $(RP)_2Mo_5$ anions on the chain (1) coordinate to the Co2 ions of ladder chains (2, 3). In this way, a complicated layer forms and parallels the *ab* plane (Figure 2)

If the $(RP)_2Mo_5$ anions and Co1 ions are considered as the three connection nodes and Co2 as the four connection node, the layer can be described using a topological symbol ($8^4 \times 8^3 \times 8^3$) (Figure 3).

There are many hydrogen bonds between oxygen atoms (O1, O3, O23, O24, O25) of the $(RP)_2Mo_5$, carboxyl oxygen atoms (O21, O22), nitrogen atom of protonated bipy (N5), coordination water molecules (O1W, O2W, O3W), and lattice water molecules (OW1−OW6, Table S2, Supporting Information), in which hydrogen bonds, O21H21B(layer1)···OW2HW2C···O23(layer2) and O22H22B(layer1) ···OW4H10J···O25(layer3), links these 2-D layers into a 3-D

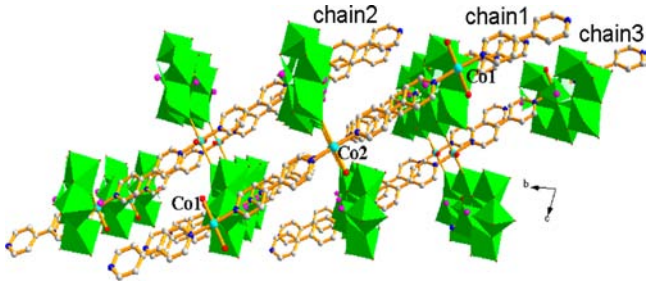

Figure 2. Layer structure of **1**. All hydrogen atoms, lattice water, and propyloic groups are omitted for clarity.

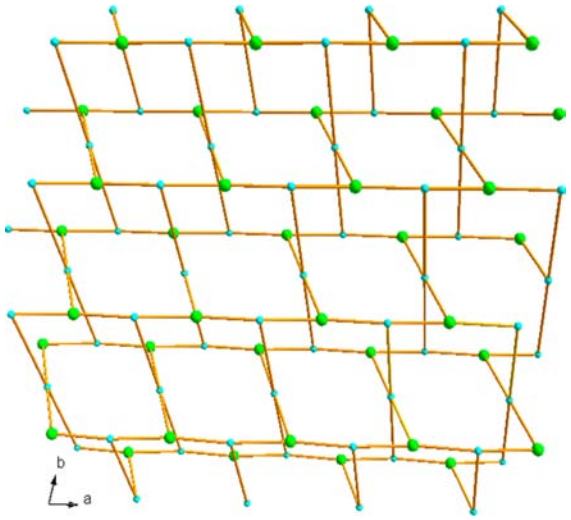

Figure 3. Topology framework of **1** with ($8^4 \times 8^3 \times 8^3$).

structure (Figure S2, Supporting Information). The protonated bipy molecular ions are linked with $(RP)_2Mo_5$ by hydrogen bonds, N5H5B···OW1H10L···O24.

$[Fe_3(bipy)_4(H_2O)_6\{(HO_2C_3H_4PO_3)_2Mo_5O_{15}\}_2]\cdot(H_2bipy)_2\cdot 18H_2O$ (***2***). The crystal structure of compound **2** was not solved from diffraction data due to the poor crystal quality, but its IR spectrum and experimental XRPD pattern were very similar to that of **1** (Figure S3, Supporting Information), indicating that compound **2** has the same framework structure as **1**.

$[Cu(bipy)(H_2O)_2\{(HO_2CC_2H_4PO_3)_2Mo_5O_{15}\}]\cdot(H_2bipy)\cdot 4H_2O$ (***3***). Compound **3** consists of one copper(II) ion, one $[(HO_2CC_2H_4PO_3)_2Mo_5O_{15}]^{4-}$ anion, two 4,4′-bipy molecules, and six water molecules as shown in Figure S4, Supporting Information. The $[(HO_2CC_2H_4PO_3)_2Mo_5O_{15}]^{4-}$ anion of **3** is identical to that of **1**, but it acts as a bidentate ligand and its two terminal oxygen atoms (O13, O28) connect with Cu1 and Cu1′ ions, respectively. The propyloic groups do not take part in the coordination to the Cu ions. The six-coordinated Cu1 ion is located in an elongated octahedral center (Table S1, Supporting Information), combining two terminal oxygen atoms of two $(RP)_2Mo_5$ anions, two nitrogen atoms (N1, N3) of two bipy molecules, and two water molecules.

The bipy molecule bridges Cu1 ions with its N1 and N3 atoms, forming a 1-D coordination polymer chain (CuL) extending along the *b* axis. $(RP)_2Mo_5$ anion also acts as a bridging ligand and coordinates with Cu1 ions of the two chains, connecting the 1-D chains into a layer parallel to the *ab* plane (Figure 4a). The fact that donor atoms of the three kinds of ligands ($(RP)_2Mo_5$, H_2O, bipy) are all in trans positions of

dx.doi.org/10.1021/ic401726a | *Inorg. Chem.* 2013, 52, 11422−11427

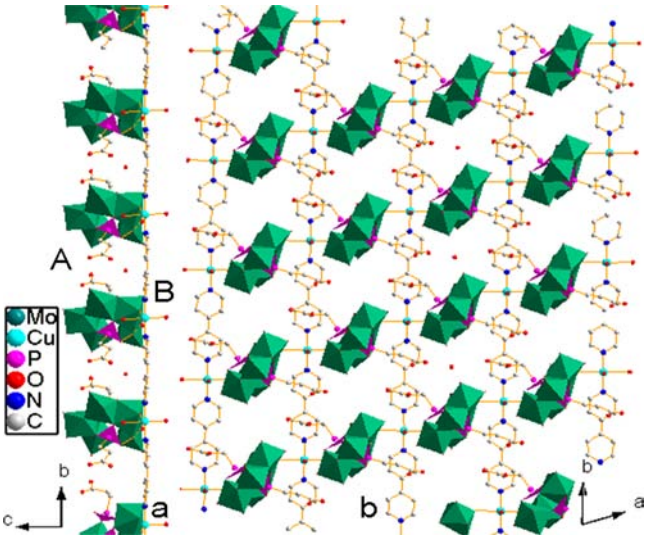

Figure 4. Views of the layer structure of **3**. Hydrogen atoms and lattice water molecules are omitted for clarity.

the CuO_3N_3 octahedron leads to two obviously different faces of the layer. Assigning the P_2Mo_5 side as A side and CuL side as B side (Figure 4b), the A side is a negatively charged surface and the B side is composed of complex cations with coordinated water molecules extending outward. These layers are arranged according to the AB−BA−AB−BA pattern. Between the B sides, the hydrogen bonds between coordinated water molecules (O2WH40B) and $(RP)_2Mo_5$ (O25) are formed; two A sides are linked by hydrogen bonds between scattered protonated bipy molecular ions and $(RP)_2Mo_5$, O10···H3BN3(bipy)N3′H3B′···O10′, and between scattered protonated bipy molecular ions, $(RP)_2Mo_5$, and crystal water molecules, O7···H98AOW2···H4BN4(bipy)N4′H4B′ ··· OW2′H98A′···O7′ (Figure 5 and Table S2, Supporting Information), that is, it is the hydrogen bonds that connect the layer into a three architecture of **3**.

IR Spectroscopic and Thermal Analyses. IR spectra of compounds **1**−**3** exhibit similar characteristic peaks (Figure S5a−c, Supporting Information). The characteristic bands at 922, 812, and 666 for **1**, 922, 810, and 665 for **2**, and 918, 802, and 669 for **3** are attributed to ν(Mo−O) and ν(Mo−O−Mo) vibrations,[1] respectively. The bands in the 1106−986 cm^{-1} region are attributed to ν(P−O). Bands in the region 1110−1730 cm^{-1} for compounds **1**−**3** can be assigned to the characteristic peaks of the organic ligand. The asymmetric and symmetric vibrations of the carboxyl group at 1729 and 1410 cm^{-1} for **1**, 1720 and 1411 cm^{-1} for **2**, and 1717 and 1420 cm^{-1} for **3** are observed; bands at about 1600 cm^{-1} are assigned to ν(C═C) of the py ring; the vibration absorption bands of CH_2 are at about 1500 cm^{-1} for $\delta(CH_2)$ and 2950 cm^{-1} for $\nu(CH_2)$. Bands at 3050−3094 cm^{-1} are attributed to ν(C−H) of py ring. Typical bands of the water molecules are centered at 1642 and 3432 cm^{-1} for **1**, 1639 and 3437 cm^{-1} for **2**, and 1635 and 3480 cm^{-1} for **3**; the bands centered at 3383 cm^{-1} for **1**, 3386 cm^{-1} for **2**, and 3363 cm^{-1} for **3** are indicative of the presence of hydrogen bands.

To characterize the compounds more fully in terms of thermal stability, their thermal behavior was studied using thermal analysis methods. For **1** (Figure S6a, Supporting Information), weight loss (obsd 9.00%; calcd 9.01%) in the temperature range from 19 to 113 °C corresponds to removal of 18 water molecules. The second stage (obsd 7.32% ; calcd 7.34%) in the ranges of 113 °C−316 °C can be attributed to loss of six coordination water molecules and one free bipy ligands. The third weight losses of 28.58% at 316−600 °C are mainly attributed to loss of remaining bipy ligands and transformation of $(RP)_2Mo_5$ into the corresponding oxides. The DTA curve shows an endothermic peak at 88.7 °C for the first weight loss and two exothermic peaks corresponding to the second and third weight losses, respectively, at 313.4 and 575.88 °C. For **2** (Figure S6b, Supporting Information), the first weight loss of 2.98% at 19−104 °C corresponds to loss of three water molecules (calcd 3.00%). A slow weight loss of 9.80% at 104−307 °C corresponds to loss of remaining water molecules (calcd 9.01%). The following weight loss corresponds to loss of bipy ligand and transformation P_2Mo_5 unit into the corresponding oxides at 307−600 °C. The endothermic peak and exothermic peaks in the DTA curve appear, respectively, at 103 and 326 and 425 and 473 °C. For **3** (Figure S6c, Supporting Information), it loses its four lattice water molecules (obsd 3.50%; calcd 3.58%) from 55 to 115 °C; loss of three water molecules and one bipy ligand occurs at 115−434 °C (obsd 13.90%; calcd 13.94%). The third weight loss of 20.0% corresponds to loss of other bipy ligand and transformation $(RP)_2Mo_5$ into the corresponding oxides at 434−800 °C. The whole weight loss (38.29%) is very consistent with the calculated one (37.50%).

Luminescent Properties. The luminescent property of **1**−**3** was tested in the solid state at room temperature (Figure 6). In order to understand the emission of the compounds, photoluminescence spectra of $(Me_4N)_6[P_2Mo_5O_{23}]$ and 4,4′-bipyridine were cited. The P_2Mo_5 cluster displays luminescence with two main emission peaks at 410 (a broad emission) and 470 nm (λ_{ex} = 259 nm),[5h] which are assigned to LMCT (O → Mo) and 4,4′-bipyridine at about 444 nm (λ_{ex} = 400 nm)[8] assigned to intraligand $\pi^* \rightarrow \pi$ transition. Upon excitation at 367 nm, compounds **1** and **2** show emission peaks at 420 and 421 nm, respectively, indicating that they have a similar structure. Compared with the emissions of $(Me_4N)_6[P_2Mo_5O_{23}]$ (Figure 6), emissions of compounds **1** and **2** come mainly from that of $[(RP)_2Mo_5O_{23}]$ but shift about 10 nm toward long wavelength due to the changes in energy levels resulting from coordination of $[(RP)_2Mo_5O_{23}]$ to M ions. On the other hand, the emission intensity of **1** and **2** seems

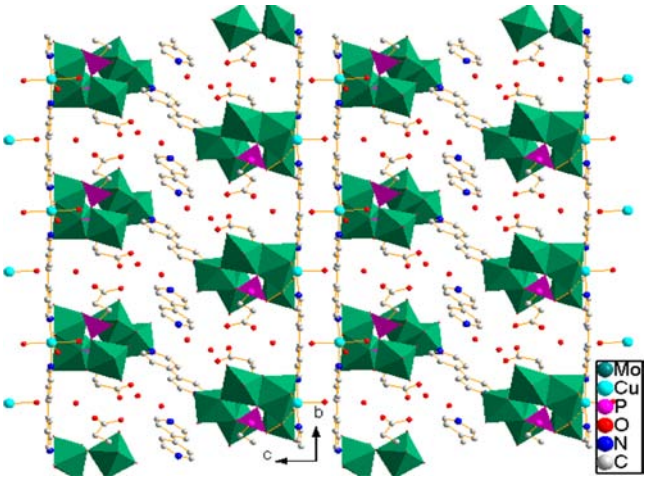

Figure 5. BA−AB−BA−AB layer arrangement of **3**. All hydrogen atoms are omitted for clarity.

dx.doi.org/10.1021/ic401726a | Inorg. Chem. 2013, 52, 11422−11427

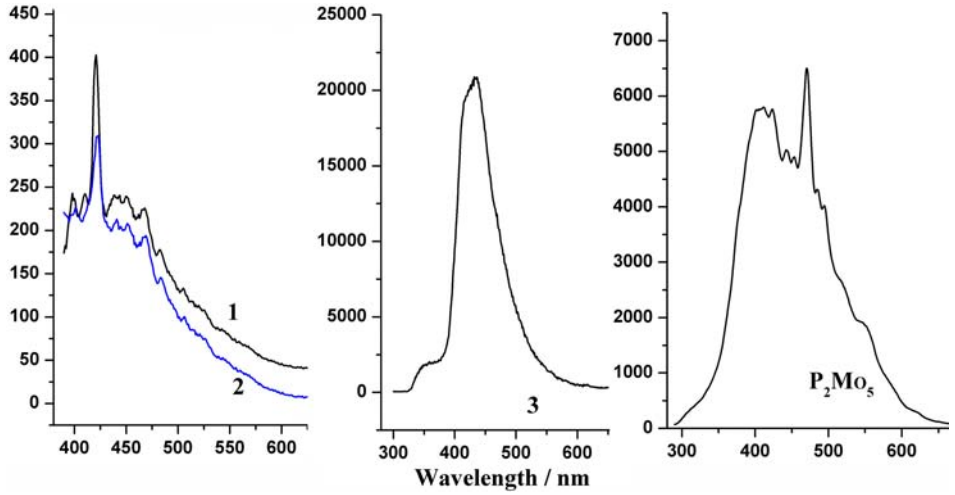

Figure 6. Emission spectra of compounds **1**−**3** and $(Me_4N)_6[P_2Mo_5O_{23}]$.

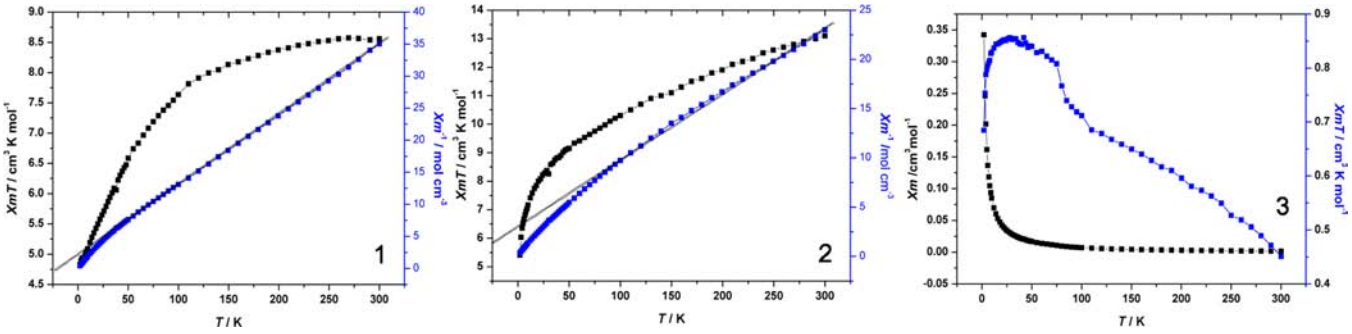

Figure 7. Temperature dependence of the $\chi_m T$ and $1/\chi_m$ (χ_m for **3**) of compounds **1**−**3**.

reduced, that is, coordination of $[(RP)_2Mo_5O_{23}]$ to M ions quenches partially LMCT (O → Mo). Compound **3** gives a broad and intensive emission band at λ_{max} = 436 nm (λ_{ex} = 280 nm). Emission of compound **3** is rather different from that **1** and **2**. The difference in the photoluminent behavior of **1**−**3** can be explained by their structures. In **1**−**3** there exist protonated bipy molecular ions; therefore, the intensive emission of **3** cannot be attributed to the intramolecular π^* → π transition of bipy. In **3** Cu ions and bipy form an infinite Cu−bipy complex chain, the bipy rings in the Cu−bipy complex chain, and the square (*xy* plane) of CuN_2O_4 octahedron are in same plane (Figure S7, Supporting Information). Thus, the d_{xz} or d_{yz} orbital of Cu^{2+} ion in an octahedral field may overlap with the delocalized π orbital of bipy, easily producing bipy → Cu charge transition. In contrast, in compound **1**, Co ions and bipy form a trimetallic complex cation and the bipy rings and square (*xy* plane) of CoN_2O_4 octahedron are angled at about 45°, which does not favor the bipy → Cu charge transition. Its asymmetric broad band implies the coactions of several charge transfers: O → Mo transition of functionalized $(RP)_2Mo_5$[5h,9] and intramolecular π^* → π transition of bipy[8] as well as L → Cu in bipy−Cu complex, which is the main contribution to the intensive emission.

Magnetic Properties. Variable-temperature magnetic susceptibilities of **1**−**3** are shown in Figure 7 in the form of $\chi_m T$ vs *T* and $1/\chi_m$ vs *T* plots. The $\chi_m T$ products of **1** and **2** at room temperature are 8.55 and 13.10 $cm^3\ mol^{-1}\ K$ per formula unit, respectively. With the decrease of the temperature, $\chi_m T$ values of **1** and **2** continuously decrease and reach 4.83 and 5.41 $cm^3\ mol^{-1}\ K$ at 2 K, indicating an antiferromagnetic interaction. The effective magnetic moments (μ_{eff}) obtained from the equation $\mu_{eff} = 2.828(\chi_m T)^{1/2}$ are 8.20 μ_B for **1** and 10.08 μ_B for **2**, which are bigger than the calculated values of 6.79 $cm^3\ mol^{-1}\ K$ for three isolated Co^{2+} ($s = 3/2$, $g = 2.0$) and 8.48 $cm^3\ mol^{-1}\ K$ for three isolated Fe^{2+} ions ($s = 2$, $g = 2.0$), respectively. The bigger μ_{eff} values are caused by the orbital contribution for the ions with more than five d electrons. The $1/\chi_m$ vs *T* plots (Figure 7) of **1** and **2** are almost linear in the temperature range of 20−300 and 75−300 K, which are fitted well by the Curie−Weiss law with Curie constants of 9.11 $cm^3\ mol^{-1}\ K$ for **1** and 14.86 $cm^3\ mol^{-1}\ K$ for **2** and Weiss constants of −18.09 K for **1** (R^2 = 0.99885) and −45.58 K for **2** (R^2 = 0.99776). The negative Weiss constants indicate weak antiferromagnetic interactions among the neighboring M(II) ions.

For compound **3** the observed $\chi_m T$ value at 300 K is 0.45 $cm^3\ mol^{-1}\ K$ (Figure 7); with decreasing temperature, the $\chi_m T$ value continuously increases and reaches 0.86 $cm^3\ mol^{-1}\ K$ at 28 K; below 28 K the $\chi_m T$ value quickly drops to 0.68 $cm^3\ mol^{-1}\ K$ at 2 K, indicating a ferromagnetic interaction as in other Cu^{2+} complexes with linear chain structure[10a] or tetranuclear ring structure.[10b] Considering the crystal structure of **3**, the reason for ferromagnetic interaction may be drawn. In **3** the two rings of a bipy are in a plane; furthermore, the plane of bipy rings in the CuL complex chain and the square (*xy* plane) of CuN_2O_4 octahedron are in same plane. Thus, the d_{xz} or d_{yz} orbital of Cu^{2+} ion in an octahedral field may overlap with the delocalized π orbital of bipy, performing the ferromagnetic exchange. In contrast, in compound **1** the bipy ring plane and the square (*xy* plane) of CoN_2O_4 octahedron are

dx.doi.org/10.1021/ic401726a | *Inorg. Chem.* 2013, 52, 11422−11427

angled at about 45°, which does not favor magnetic exchange, so compound **1** only exhibits simple antiferromagnetic interaction.

CONCLUSION

Functionalized Strandberg-type polyoxometalate-based inorganic−organic compounds could be prepared in aqueous solution. Functionalized Strandberg-type polyoxometalate $[(HO_2CC_2H_4PO_3)_2Mo_5O_{15}]^{4-}$ anions formed in situ act as tridentate ligand in **1** and **2** or bidentate ligand in **3** and link metal ions together with bipy, forming different 2-D frameworks. The different 2-D frameworks lead to different photoluminescent emissions and magnetic exchange, that is, the infinite polymeric chain with a coplane of bipy rings and square of CuN_2O_4 octahedron leads to the intense emission and ferromagnetic change.

ASSOCIATED CONTENT

Supporting Information

Additional information as noted in the text. This material is available free of charge via the Internet at http://pubs.acs.org.

AUTHOR INFORMATION

Corresponding Author

*E-mail: chenyg146@nenu.edu.cn.

Notes

The authors declare no competing financial interest.

REFERENCES

(1) Strandberg, R. *Acta Chem. Scand.* **1973**, *27*, 1004−1018.

(2) (a) Hedman, B. *Acta Chem. Scand.* **1973**, *27*, 3335−3354. (b) Kwak, W.; Pope, M. T.; Scully, T. F. *J. Am. Chem. Soc.* **1975**, *97*, 5753−5738. (c) Stalick, J. K.; Quicksall, C. O. *Inorg. Chem.* **1976**, *15*, 1577−1584. (d) Hedman, B.; Strandberg, R. *Acta Crystallogr.* **1979**, *B35*, 278−284. (e) Pettersson, L.; Andersson, I.; Öhman, L.-O. *Acta Chem. Scand.* **1985**, *A39*, 53−58. (f) Pettersson, L.; Andersson, I.; Öhman, L.-O. *Inorg. Chem.* **1986**, *25*, 4726−4733. (g) Yagasaki, A.; Andersson, I.; Pettersson, L. *Inorg. Chem.* **1987**, *26*, 3926−3933. (h) Ozeki, T.; Ichida, H.; Miyamae, H.; Sasaki, Y. *Bull. Chem. Soc. Jpn.* **1988**, *61*, 4455−4457. (i) Lyxell, D.-G.; Strandberg, R. *Acta Crystallogr.* **1988**, *C44*, 1535−1538. (j) Lyxell, D.-G.; Strandberg, R.; Boström, D.; Pettersson, L. *Acta Chem. Scand.* **1991**, *45*, 681−686. (k) Lowe, M. P.; Lockhart, J. C.; Clegg, W. P.; Fraser, K. A. *Angew. Chem., Int. Ed.* **1994**, *33*, 451−454. (l) Lowe, M. P.; Lockhart, J. C; Forsyth, G. A.; Clegg, W.; Fraser, K. A. *J. Chem. Soc., Dalton Trans.* **1995**, 145−152. (m) Inoue, M.; Yamase, T. *Bull. Chem. Soc. Jpn.* **1996**, *69*, 2863−2869. (n) W, T.; Harrison, A.; Dussack, L. L.; Jacobson, A. J. *Acta Crystallogr., Sect. C: Cryst. Struct. Commun.* **1997**, *53*, 856−859. (o) Lyxell, D.-G.; Boström, D.; Hashimoto, M.; Pettersson, L. *Acta Chem. Scand.* **1998**, *52*, 425−430. (p) Mayer, C. R.; Marrot, J.; Se′cheresse, F. *J. Mol. Struct.* **2004**, *704*, 59−62. (q) Carraro, M.; Sartorel, A.; Scorrano, G.; Maccato, C.; Dickman, M. H.; Kortz, U.; Bonchio, M. *Angew. Chem., Int. Ed.* **2008**, *47*, 7275−7279.

(3) (a) Kortz, U.; Marquer, C.; Thouvenot, R.; Nierlich, M. *Inorg. Chem.* **2003**, *42*, 1158−1162. (b) Burkholder, E.; Golub, V.; O'Connor, C. J.; Zubieta, J. *Inorg. Chem.* **2003**, *42*, 6729−6740. (c) Chubarova, E. V.; Klöck, C.; Dickman, M. H.; Kortz, U. *J. Cluster Sci.* **2007**, *18* (3), 698−710.

(4) (a) Finn, R. C.; Burkholder, E.; Zubieta, J. *Chem. Commun.* **2001**, 1852−1853. (b) Finn, R. C.; Zubieta, J. *Inorg. Chem.* **2001**, *40*, 2466−2467. (c) Finn, R. C.; Rarig, R. S., Jr.; Zubieta, J. *Inorg. Chem.* **2002**, *41*, 2109−2123. (d) Burkholder, E.; Zubieta, J. *Inorg. Chim. Acta* **2004**, *357*, 1229−1235. (e) Burkholder, E.; Golub, V.; O'Connor, C. J.; Zubieta, J. *Inorg. Chem.* **2004**, *43*, 7014−7029. (f) Zhang, H.-S.; Fu, R.-B.; Zhang, J.-J.; Wu, X.-T.; Li, Y.-M.; Wang, L.-S.; Huang, X.-H. *J. Solid State Chem.* **2005**, *178*, 1349−1355. (g) Fu, R.-B.; Wu, X.-T.; Hu, S.-M.; Zhang, J.-J.; Fu, Z.-Y.; Du, W.−X.; Xia, S.-Q. *Eur. J. Inorg. Chem.* **2003**, 1798−1801. (h) Burkholder, E.; Golub, V.; ÓConnor, C. J.; Zubieta, J. *Chem. Commun.* **2003**, 2128−2129. (i) Gabriel Armatas, N.; Allis, D. G.; Prosvirin, A.; Carnutu, G.; ÓConnor, C. J.; Dunbar, K.; Zubieta, J. *Inorg. Chem.* **2008**, *47*, 832−854. (j) Armatas, N. G.; Ouellette, W.; Whitenack, K.; Pelcher, J.; Liu, H.; Romaine, E.; ÓConnor, C. J.; Zubieta, J. *Inorg. Chem.* **2009**, *48*, 8897−8910. (k) Bartholomä, M.; Chueng, H.; Pellizzeri, S.; Ellis-Guardiola, K.; Jones, S.; Zubieta, J. *Inorg. Chim. Acta* **2012**, *389*, 90−98.

(5) (a) Lu, J. J.; Xu, Y.; Goh, N. K.; Chia., L. S. *Chem. Commun.* **1998**, 2733−2734. (b) Burkholder, E.; Zubieta, J. *Chem. Commun.* **2001**, 2056−2057. (c) Weng, J.; Hong, M.; Liang, Y.; Shi, Q.; Cao, R. *J. Chem. Soc., Dalton Trans.* **2002**, 289−290. (d) Lu, Y.; Li, Y. G.; Wang, E. B.; Lü, J.; Xu, L.; Clérac, R. *Eur. J. Inorg. Chem.* **2005**, 1239−1244. (e) Lu, Y.; Lü, J.; Wang, E. B.; Guo, Y. Q.; Xu, X. X.; Xu, L. *J. Mol. Struct.* **2005**, *740*, 159−163. (f) Burkholder, E.; Zubieta, J. *Chem. Commun.* **2001**, 2056−2057. (g) Yu, K.; Zhou, B. B.; Yu, Y.; Su, Z. H.; Wang, H. Y.; Wang, C. M.; Wang, C. X. *Dalton Trans.* **2012**, *41*, 10014−10020. (h) Zhang, C.-X.; Chen, Y.-G.; Q, T.; Zhang, Z.-C.; Liu, D.-D.; Meng, H.-X. *Inorg. Chem. Commun.* **2012**, *17*, 155−158. (i) Lu, X. M.; Wang, X. J.; Li, P. Z.; Pei, X. H.; Ye, C. H. *J. Mol. Struct.* **2008**, *872*, 129−134. (j) Niu, J.; Ma, J.; Zhao, J.; Ma, P.; Wang, J. *Inorg. Chem. Commun.* **2011**, *14*, 474−477.

(6) Jones, S.; Zubieta, J. In *Metal Phosphonate Chemistry: From Synthesis to Applications*; Clearfield, A ., Demadis, K., Eds.; Royal Society of Chemistry: Cambridge, 2012; pp 192−234.

(7) Sheldrick, G. M. *SHELXS97, Program for Crystal Structure Solution*; University of Göttingen: Göttingen, 1997.

(8) Cha, Y.-E.; Li, X.; Liang, H. *Polyhedron* **2013**, *50*, 208−214.

(9) (a) Yamase, T.; Sugeta, M. *J. Chem. Soc., Dalton Trans.* **1993**, 759−764. (b) Ito, T.; Yashiro, H.; Yamase, T. *Langmuir* **2006**, *22*, 2806−2810.

(10) (a) Klein, C. L.; Majeste, R. J.; Trefonas, L. M.; O'Connor, C. J. *Inorg. Chem.* **1982**, *21*, 1891−1897. (b) Cull, J. E.W.; Habib, F.; Korobkov, I.; Murugesu, M.; Scott, J. *Inorg. Chim. Acta* **2011**, *370*, 98−101.